A PASSIVE DEVICE FOR POSTMORTEM DETUMBLING / ANTITUMBLING OF LEO SATELLITES, TO FACILITATE ACTIVE REMOVAL

Maxime Senes[(1)], Kristen Lagadec[(1)], Baptiste Brault[(1)], Bertrand Raffier[(2)], Adrien Dias Ribeiro [(2)]

[(1)]Airbus Defence and Space, Toulouse, France, maxime.senes@airbus.com, kristen.lagadec@airbus.com, baptiste.brault@airbus.com
[(2)]CNES, Toulouse, France, bertrand.raffier@cnes.fr, adrien.diasribeiro@cnes.fr

ABSTRACT

To limit the risk of cascading collisions, we will need active debris removal missions to retrieve satellites that die before they can be deorbited. It is well understood that sudden fatal failures can cause a dead satellite to tumble uncontrollably, but even properly decommissioned satellites may start tumbling spontaneously from solar radiation pressure torque buildup, making capture extremely challenging in both cases. The availability of a detumbling/antitumbling device ensuring passive stabilization of dead satellites could greatly reduce the risk and cost of debris removal missions.

We describe a passive magnetic damping device attached to a satellite's structure, which dissipates the kinetic energy and angular momentum thanks to eddy currents resulting from differential angular rates between the satellite and the Earth's magnetic field, eventually stopping the tumbling motion.

Detailed sizing and simulation activities have demonstrated that one such small and lightweight device is capable of detumbling a medium-to-large satellite within just a few weeks, while also preventing self-tumbling. The paper reviews the current development status, from initial sizing to performance simulations and vibration tests of two prototypes. These steps pave the way for the final development stages of a universally available detumbling function that can be a game-changer for active debris removal.

1 CONTEXT AND PROPOSED SOLUTION

1.1 Active debris removal and tumbling debris

To limit the rate of cascading collisions between space debris (Kessler syndrome), post-mission disposal will not be enough. Statistically, *some* satellites will remain stranded. This is even more critical with (and especially *within*) large constellations. Sustainable access to low earth orbits will require Active Debris Removal (ADR), to curb the runaway collision risk [1].

However, the extreme challenges of capturing debris with potentially large tumbling rates have been holding back initiatives and impeding the prospects of a viable business model for ADR.

There are essentially three reasons for which a derelict satellite or piece of debris might be tumbling:

- A fatal failure causing the loss of the mission, as well as significant dynamics (e.g. propulsion failure)

- A catastrophic event occurring after the end of the mission (a collision with a smaller piece of debris, or an explosion in case electrical or fluidic passivation was incomplete)
- The slow and steady buildup of angular momentum from accumulation of tiny external perturbations (e.g. an asymmetry in solar radiation pressure torque, similar to the YORP effect on asteroids), even after the satellite is properly decommissioned.

Any significant tumbling rates make all ADR operations much more challenging. The need to be able to cope with angular rates upwards of 3 deg/s has made prospective ADR mission designs very complex, and in general has been holding back ADR development initiatives.

1.2 Expected benefits from a detumbling function

A detumbling function with the capability to guarantee very low angular rates (< 0.2 deg/s) would make active debris removal of future LEO missions much less challenging:

- The chaser vehicle can be smaller (it does not have to struggle with the large momentum of the target debris)
- Proximity operations are much safer, with the possibility to match the chaser's trajectory and attitude to the target's angular motion
- The capture system can be much simpler, inspired from existing designs for cooperative or semi-cooperative rendezvous
- Relative navigation is simplified, since the motion of the target is much less chaotic
- The post-capture transient is a lot smoother, with only modest momentum residuals to transfer and dump.

1.3 Operating principle of the DETUMBLER[1]

The detumbling solution developed by Airbus is a fully passive device involving a rotor fitted with magnets, which is free to pivot inside an aluminium housing (the stator), itself attached to the structure of the satellite. Even when the satellite is tumbling, the rotor tends to remain aligned towards the local geomagnetic field. Because the rotor magnets are very close to the stator wall, the difference in angular rates between the stator and rotor creates eddy currents in the stator's conductive material. These in turn lead to a resistive viscous torque opposing the rotation.

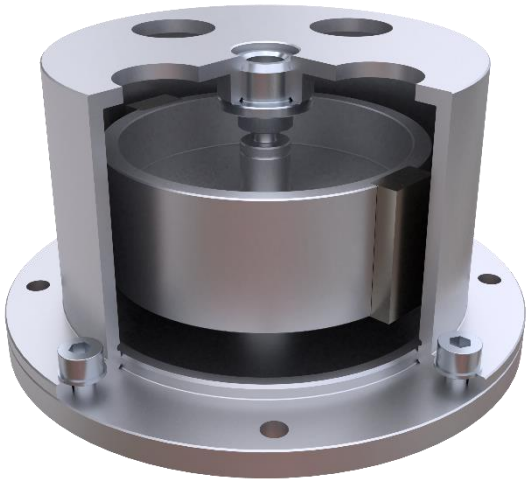

Figure 1: 3D rendering of the DETUMBLER – approximately to scale (rotor diameter = 5cm)

[1] Device for Eliminating Tumbling or other Unwanted Motion Before the Launch of an Economical Remover

1.4 Intended missions

The altitude range most penalized by the accumulation of space debris extends from typically 550 km to 1200 km. Orbits below 500 km are self-cleaning, with air drag naturally deorbiting debris in less than 25 years. Above 1200 km the population of satellites is currently too scarce to be of any concern.

Therefore, the device is intended to cover the low orbits, where the Earth's magnetic field has substantially the same magnitude as at ground level, justifying the operating principle. All possible values of orbit inclinations are covered, including equatorial orbits for which the comparatively lower detumbling efficiency will simply translate into longer convergence times.

In terms of spacecraft sizes, the intention is to cover as wide a scope as possible with a single design, from smallsats to medium-large satellites. The key parameter in terms of detumbling efficiency is inertia, which can range from less than 1 kg.m² for smaller satellites, up to and above 100,000 kg.m² for the biggest ones. For the initial design, we have chosen to set the upper bound at 5000 kg.m², which typically corresponds to a 1.5-ton satellite, covering more than 95% of the current distribution of satellites in flight[2].

2 REQUIREMENTS AND SIZING

2.1 Main functional requirements

Time constant and damping coefficient. When starting from an initially tumbling state, the angular rates follow an exponential decay law, with a time-constant τ depending on the satellite's moment of inertia and on the rotor's equivalent viscous damping coefficient k_v through:

$$\tau = \frac{I_{sat}}{k_v} \qquad [1]$$

This time-constant needs to be small with respect to the time it takes for an active debris removal mission to be put together and launched, which will reasonably not be less than a few years. A value of τ = 100 days is thus considered as a realistic requirement for the detumbling time-constant, (reducing angular rate by a factor 20 in less than a year). This in turn requires a damping coefficient of 1 mNms/rad. This value also covers antitumbling for the vast majority of satellites.

Saturation rate. Above a certain differential rate between the rotor and stator, the viscous torque exceeds the magnetic torque and the rotor no longer remains aligned with the magnetic field.

$$M \times B = k_v \cdot \omega_{max} \qquad [2]$$

In this *saturated* regime, the reduction of angular momentum is no longer exponential but simply linear. Although preferably avoided, saturation certainly does not prevent detumbling, it only delays it. A target value of ω_{max} = 3 deg/s has been chosen for the saturation rate.

[2] There is however no physical obstacle for deriving a larger detumbler for much bigger satellites, should the need arise.

2.2 Limiting disturbances to the host spacecraft during the mission

Since the device is fully passive and does not have any clamping mechanism, it is already functional during the mission. It must therefore be designed so as to avoid causing noticeable disturbances on the host spacecraft. This sizing exercise is first conducted for the upper bound of the range (larger inertia and corresponding damping coefficient k_v = 1 mNms/rad), but the process for deriving an alternate sizing for smaller satellites is summarized in §4.5.

Disturbance torque. A threshold of 50 µNm is considered as an acceptable level of disturbance[3] that the host may experience without requiring specific ADCS analyses. The device causes two types of disturbance torques: axial viscous torque, due to the damping effect; and transverse magnetic torque, when the magnetic field is not in the plane of the rotor. For the former, it can easily be verified that with k_v = 1 mNms/rad, it would take a slew rate of 3 deg/s to reach the acceptable limit, which is a rate that only the most agile spacecraft can reach. Limiting the latter to 50 µNm imposes a limitation of $M < 1.6$ Am² for the magnetic moment of the rotor (the sum of the magnetic moment of the two magnets), considering a typical value of 30 µT for the magnetic field in LEO.

Magnetic compatibility. The magnetic moment carried by the rotor can perturb the surrounding magnetic field. This could become an issue if the detumbler was accommodated too close to a magnetometer, for instance. Conversely, the detumbler should not be accommodated too close to permanent magnets or magnetized parts, so that the local magnetic field indeed follows the Earth's. An indicative value of 3 µT (bias < $B_0/10$) is considered as the acceptable level of perturbation in both cases. For large satellites (where the detumbler's magnetic moment is 1.6 Am²), this imposes a clearance of 40 cm between the detumbler and a magnetometer. But since these disturbances decrease as the distance cubed, reducing the bias even further would not require much more space.

2.3 Mechanical and environment requirements

- *Mass and size*. Since the same device is intended for a large range of satellites including smaller ones, it must be very small and lightweight. The target is 5.5 cm (2") in diameter and 5 cm (1½") in height for size, and 100 grams (3.5 oz) in mass, with a goal of 50 grams.
- *Dry friction* is a key design driver: it needs to be significantly lower than the magnetic torque so that the rotor can follow the magnetic field without remaining stuck (including when *B* is not in the plane of the rotor). Dry friction in orbit must therefore be less than 5 µNm.
- *Testability under 1g*. Being able to verify the damping coefficient and the level of dry friction under gravity is also a major design driver, as it requires the dry friction under load to comply with the 5 µNm requirement (even though that value is only actually required in flight).
- *Launch environments*. The detumbler must withstand launch loads (vibration/shocks) for all possible launchers and spacecraft accommodations. The typical levels required from equipment suppliers are thus applicable.
- *Thermal environment* in flight. In the absence of thermal control once the spacecraft is powered off, the detumbler will encounter extreme thermal conditions. It might be mounted on a wall that always faces the sun, or always faces cold space, leading a very large range of possible temperatures. The target temperature range for qualification is thus [-100°C +80°C].
- *Lifetime*. The detumbler will not only have to survive until the end of the satellite's (possibly extended) lifetime, but it will also have to remain operational until an ADR mission is sent. Fortunately, once the satellite is detumbled, the rotor will not see more than 16 cycles a day: after 100 years, this still represents much fewer than 1M cycles (with infinitesimal contact efforts)

[3] This is an order of magnitude below the typical value of disturbance torques in LEO for small-to-medium satellites

2.4 Sizing approach

The sizing approach comprises three incremental steps: analytical approximations, numerical simulations, and experimental verification.

The *analytical* step simplifies the problem into an ideal geometry, with an infinite magnet height and length and zero air gap. This makes the shape of the magnetic field trivial, while reducing the Maxwell-Faraday equations for computing the eddy currents to a 1-d differential equation with a simple closed-form solution. The expression for the ideal value of the damping coefficient is thus:

$$k_v^{\infty} = \frac{V B_r^2 r^2}{4\rho} \qquad [3]$$

(where V is the total volume of the magnets, B_r is the remanence of the magnet's material, r is the radius of the rotor, and ρ is the resistivity of the housing)

This first step allows to assess a first order of magnitude for the efficiency of the device vs its diameter and magnet size, while also offering valuable insights in terms of parametric sensitivity.

The *numerical step* simulates the actual 3D shape of the magnetic field for the magnets, and uses a numerical solver to compute the solution to the 2D Maxwell-Faraday equations. It allows to derive correction coefficients for the various effects causing the actual efficiency to differ from the ideal analytical formulation:

- Edge effect penalty for various (finite) aspect ratios of the magnets
- Drop in magnetic field for larger air gap sizes between the magnets and the stator wall
- Truncation due to the finite thickness of the stator wall

These multiplicative correction factors are then applied to the ideal analytical formulation, allowing to predict the performance and iterate between design variants without having to go through the CPU-hungry solvers.

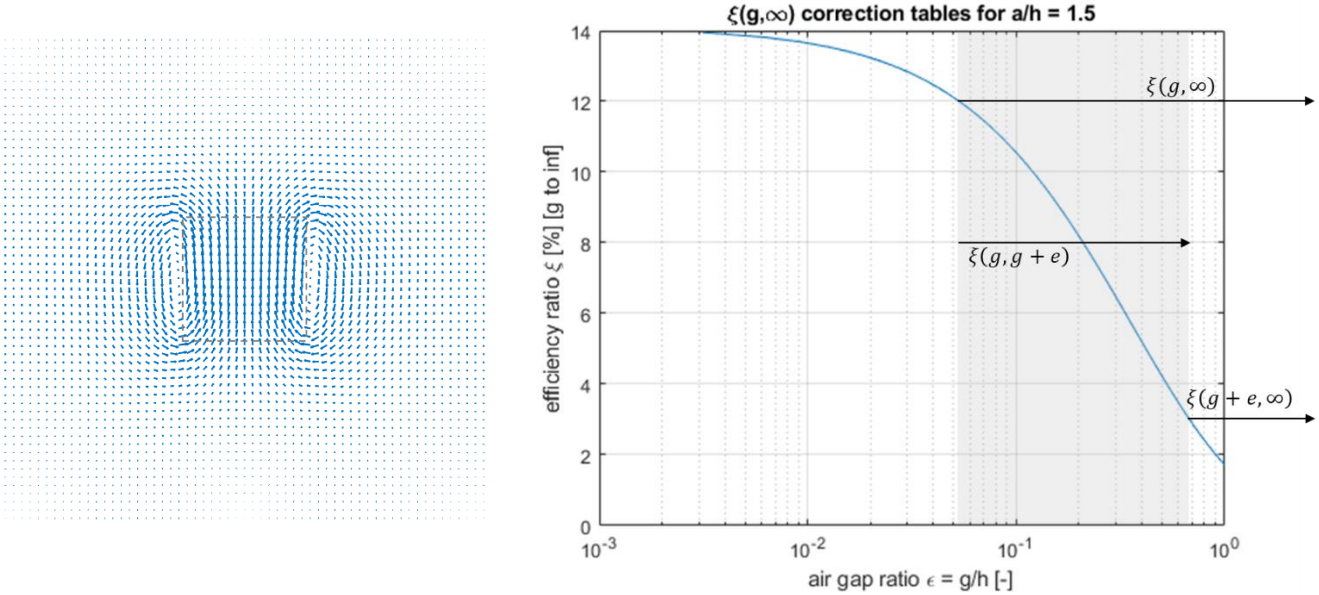

Figure 2: eddy current pattern with the edge effects for a square aspect ratio (left) correction ratio for air gap size and wall thickness (right)

The *experimental step* then consists in verifying the predictions of the former two approaches in various settings: tests on simplified 1-D models allowed to consolidate the orders of magnitude, and tests on gradually more representative breadboards allowed to calibrate the predictions more finely.

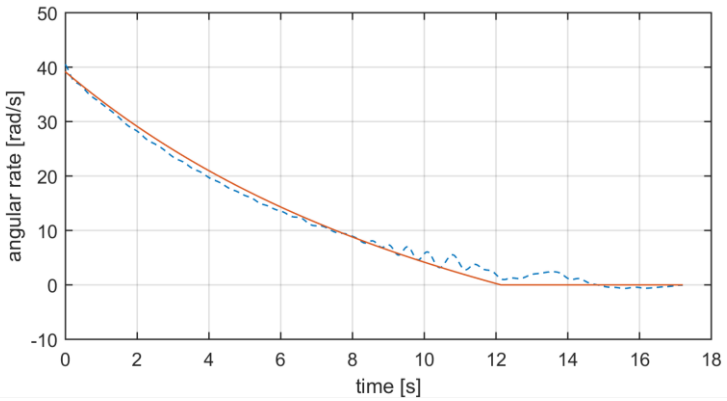

Figure 3: clear acrylic breadboard (left) / fitting an exponential decay to experimental data (right)

2.5 Final specifications

The table below recapitulates the specifications of the detumbler on which the performance campaign and the detailed design for the various prototypes and engineering models is based.

Table 1: Detumbler specifications / provisional datasheet

Mass	< 100 grams
Size	h50mm ⌀60mm
Orbits	up to 2000 km, all inclinations
Satellite inertia	up 5000 kg.m² (~1.5 tons)
Detumbling time	< 300 days
Damping ratio	up to 1 mNms/rad
Magnetic moment	< 1.6 Am²
Dry friction	< 5 µNm (goal 1 µNm)
S/C rate after detumbling	< 0.2 deg/s
Service life	> 20 years (target = 100 years)
Temperature range	−100° C to + 80°C
Power	0W (100% passive)
Disturbance torque on S/C	< 50 µNm
Accommodation constraints	> 40 cm from MAG[4]
Units needed per S/C	1

[4] This is for the 1 mNms/rad version (I_{sat} = 5000 kg.m²). The clearance shrinks to 15 cm for versions with a lower k_v

3 PERFORMANCE SIMULATION CAMPAIGNS

Once the detumbler sizing was stabilized, we conducted extensive simulation campaigns to confirm the detumbling and antitumbling performance of the device, with various assumptions on the host spacecraft. This allowed to verify that the exponential decay behavior was indeed observed with the complete 3-axis dynamics and a representative geomagnetic field model, and that the observed convergence time was consistent with the design time-constant.

3.1 Simulator setup

Since these campaigns have to cover a large number of very long simulation scenarios (several months), the simulator needs to be as efficient as possible. The models are stripped down to the bare minimum that captures the phenomena relevant to the analysis:

- A semi-analytical orbit model including the J2 effects (especially the drift of the right ascension of the ascending node, for heliosynchronous or drifting orbits).
- A magnetic field model (order 10, degree 10 using IGRF-10 data), using the current orbital position and current satellite attitude to compute the magnetic field in body frame.
- Gravity gradient torque
- Solar radiation pressure torque
- Magnetic torque from residual magnetic bias in the satellite
- The model of the detumbler itself, including the dynamics of the rotor. The transverse magnetic torque is directly applied to the spacecraft, while the axial torque accelerates the rotor, causing a friction torque (viscous and dry) which is transmitted to the spacecraft.
- The dynamics of the spacecraft is assumed rigid, since all phenomena are quite slow.
- Aerodynamic torque is not modelled, since the device is to be used at altitudes where drag is too low to bring the satellite down in 25 years.

Specific care was taken for verifying that despite the very long simulation time, the ODE solver settings did not introduce numerical drift that would invalidate the predictions. In particular, in the absence of any damping, the simulated angular momentum and kinetic energy needed to remain constant, to be sure that the simulator did not introduce artificial damping (positive or negative). Regardless, the chaotic nature of the dynamics (nonlinear, coupled, lightly damped) make the simulations essentially non-repeatable: tiny perturbations on the initial conditions lead to very different outcomes in the detailed attitude profiles. Only the macroscopic indicators (kinetic energy, momentum, average angular rate etc.) are relevant.

3.2 Behaviour analyses

A few dedicated campaigns were conducted, to illustrate specific behaviours of the dynamical system:

Three classes of converged state. When either one of the satellite's magnetic bias or gravity gradient torque significantly dominates, the final dynamics will respectively correspond to a magnetic capture (with the satellite behaving like the needle of a compass) or a gravity-gradient capture (with the axis of minimum inertia pointing up or down). However, the simulations identify a very large middle-ground for intermediate cases, where the converged state is neither of the above, but a chaotic alternation between both. In any case, the steady-state angular rates are below 0.2 deg/s, ensuring that even if the attitude motion is chaotic in the long run, it is slow enough for safe capture.

Saturated regime. Contrary to the 1-axis ideal model where saturation is a binary phenomenon, in the 3-axis case the transition between the saturated regime and the exponential regime is progressive. We could however confirm that when starting from angular rates exceeding the design value for saturation (5 deg/s instead of 3 deg/s), the initial convergence was indeed slower, with an inflexion point when the angular rate went below 3 deg/s, followed by an exponential decay as per design.

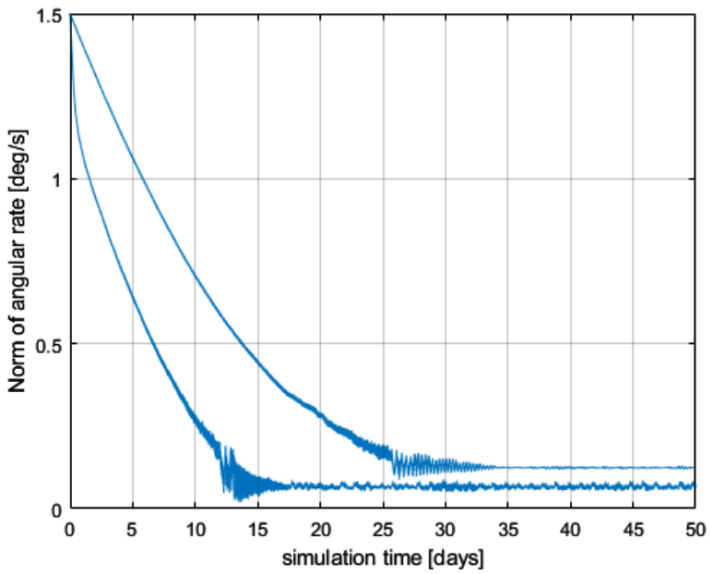

Figure 4: Comparison of two simulation cases with gravity gradient capture vs magnetic capture
The lower rate case corresponds to the gravity gradient capture, with an angular rate matching the orbital rate (0.06 deg/s), while the angular rate in the magnetic capture case is roughly double that value (0.12 deg/s) since the magnetic field points north twice per orbital revolution.

Antitumbling efficiency. In addition to damping angular rates after upsets, the detumbler is also intended as a means of preventing spontaneous spin-up from accumulation of asymmetric solar radiation pressure torque. In these campaigns, we showed how the disturbance torque acting on a few spacecraft geometries with significant asymmetry can lead to an indefinite divergence of the angular momentum, and how a detumbler prevents the phenomenon.

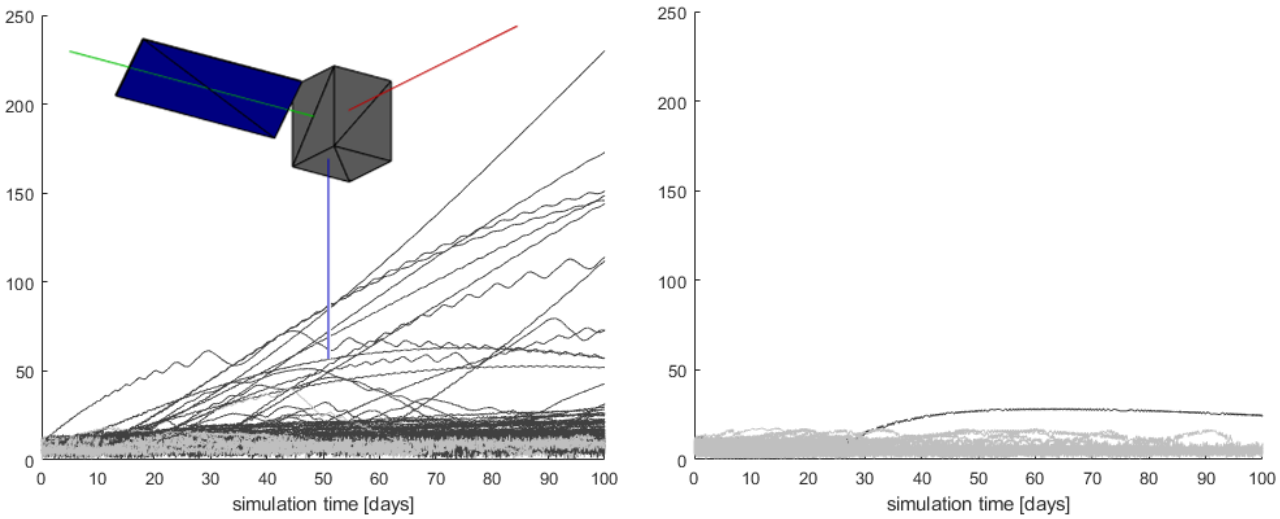

Figure 5: Angular momentum (in Nms) vs time, on an asymmetric S/C without vs with detumbler
In the absence of damping, an asymmetric spacecraft can self-tumble up to several 100 Nms in a few months (simulation campaign on the left, with random initial attitudes). By contrast, adding a detumbler[5] prevents against spontaneous spin-up.

[5] Note that in this specific instance, the large asymmetry due to the single 8-m² wing would require k_v = 5 mNms/rad

3.3 Sensitivity analyses

Additional campaigns were conducted to verify a few important sensitivities:

- Sensitivity to *dry friction*: this allowed to determine that modest levels of dry friction up to 15 µNm were mostly innocuous, but that the efficiency drops sharply beyond those values (reduction by half for f = 30 µNm, and a complete loss of efficiency for f = 48 µNm)
- Sensitivity to *spacecraft inertia*, confirming the linear relationship between inertia and convergence time
- Sensitivity to *orbit inclination*, showing a noticeable increase in convergence time for equatorial orbits compared to inclinations above 20 deg (consolidated in the nest section)
- Sensitivity to the *orientation of the detumbler*, confirming that mounting the detumbler with its rotor axis aligned with the axis of *maximum* inertia is optimum, while also showing that all other alignments are valid, with the worst alignment (along the axis of *minimum* inertia) only causing a 50% penalty on convergence time.
- Sensitivity to the *number of detumblers*: expectedly, unless the multiple devices are co-parallel, adding detumblers does not improve convergence time proportionally. Using 2 devices at right angles reduces detumbling time by 45%, while using 3 at right angles reduces detumbling time by 60%. Implementing multiple detumblers on a spacecraft is thus simply a question of redundancy, but mostly not performance[6].

3.4 Statistical performance and robustness results

The largest simulation campaign was aimed at demonstrating the robustness to all possible parameter settings, as well as the genericity of the detumbler with respect to satellite and orbit characteristics.

Table 2: Statistical campaign settings and assumptions

Parameter	Value	Remark
Number of cases	500	
Initial angular rate	1.5 deg/s	Random direction (uniform)
Initial attitude	random	Uniform on SO(3)
Local time of ascending node	[0 24h]	Random, uniform
Orbit inclination	[0 100 deg]	Random, uniform
Apogee altitude	[500 1200 km]	Random, uniform
Perigee altitude	[500 1200 km]	Random, uniform
Argument of perigee	[0 360 deg]	Random, uniform
Initial true anomaly	[0 360 deg]	Random, uniform
Satellite inertia Iyy	[1000 5000 kg.m²]	Random, uniform
Satellite inertia Ixx, Izz	[700 4500 kg.m²]	Random scaling factor wrt. Iyy
Residual magnetic moment	10 Am²	Random direction (uniform)
Local bias on magnetic field	[0 5µT]	Random, uniform
Initial rotor angle	[0 360 deg]	Random, uniform

[6] Caveat: for catering to larger satellites (> 5000 kg.m²), multiple units are a simpler solution than a redesigned device

The campaign covers a very wide range of satellite inertias corresponding to the medium-to-large satellites for which the design setpoint k_v = 1mNms/rad is intended. The orbits are completely randomized, including drifting orbits, equatorial orbits and elliptical orbits. The initial angular rate in this campaign is moderate[7], to be able to run 500 cases in a reasonable amount of time.

The campaign completely validates the design, demonstrating robustness and genericity. The principal observations were the following:

- *Convergence time* was 70 days on average, consistent with the 1 mNms/rad design and the range of values for satellite inertia.
- The *converged angular rate* after detumbling was consistently below 0.2 deg/s, with an average of 0.12 deg/s
- *Inertia and inclination* were understandably the two most important factors in predicting detumbling time.
- *Detumbling was successful* in 100% of simulations, even for the few outliers (large satellites on low inclination orbits) which did not quite reach convergence (within the preset stopping criteria) before the end of simulation at 200 days. Subsequent tests with a cut-off time at 500 days show that they all end up at angular rates below or around 0.2 deg/s
- *Altitude, residual magnetic moment and local magnetic bias* had a comparatively too modest influence to observe in the campaign results.

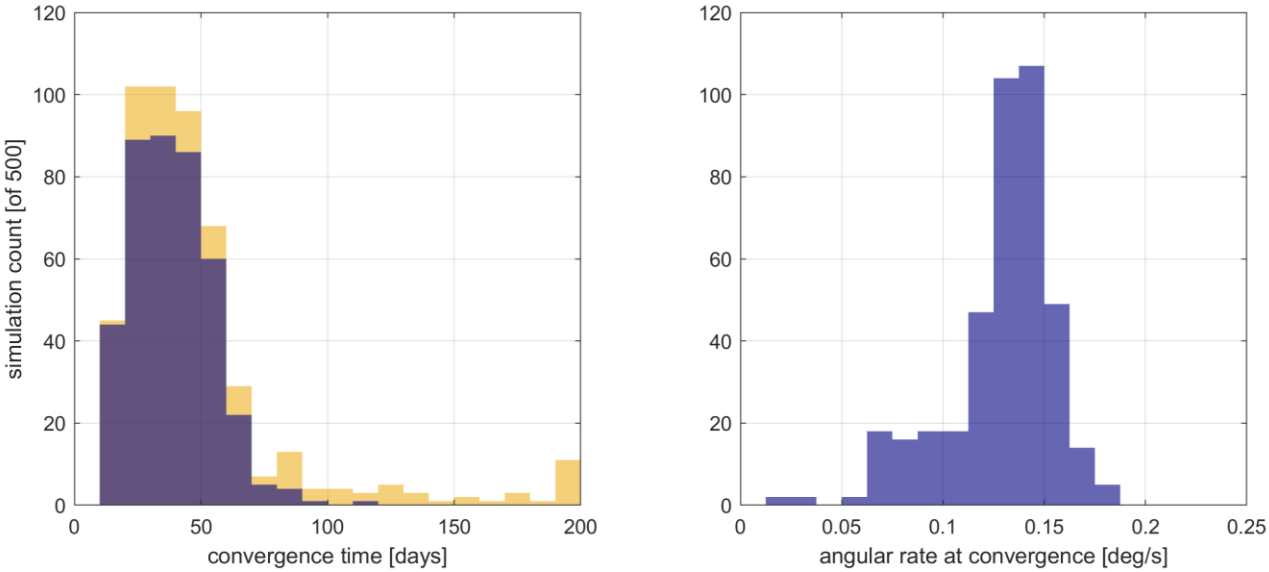

Figure 6: Distribution of convergence time (left) and converged rate (right) over 500 cases
Left: the few outliers at 200 days correspond to low inclination cases. Truncating to only inclinations above 20 deg yields the second histogram with all cases converging within 4 months. Right: the distribution appears 'bi-modal', with one big hump around 0.12 deg/s (magnetic capture) and a smaller one around 0.07 deg/s (geocentric capture).

[7] A separate campaign tested 100 cases with initial rates of 5 deg/s to demonstrate convergence despite initial saturation

4 DETUMBLER TECHNOLOGY DEVELOPMENTS

4.1 General design approach

Since the product is very simple to make, the development process relied on early prototyping and testing, with concurrent prototypes for comparing alternate design options. This allowed to converge rapidly to a general size and geometry, with very few parts.

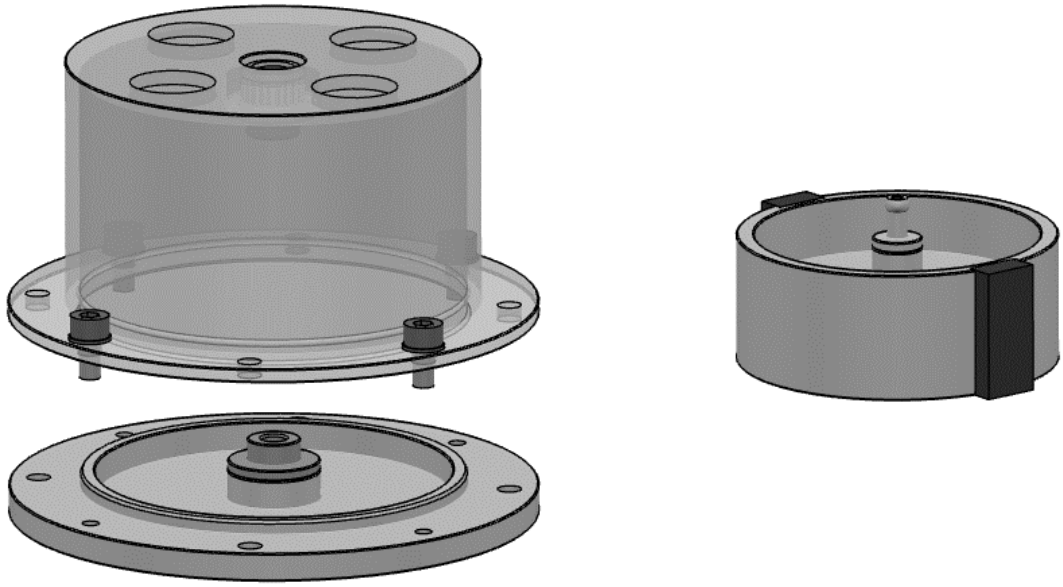

Figure 7: CAD view of the reference design (scale approximately 1:1)
The design involves the stator housing, with its bottom plate and top cover, and the rotor comprising the central axle, the rotor wheel and the magnets. The bottom plate can be indifferently attached with screws (with non-ferrous screws and inserts) or glued to the host structure.

The general design philosophy is geared towards series production: considering that the detumbler specifications are extremely generic, and taking into account the rise in mega-constellation prospects, the aim was to define a product with an extremely low recurring cost.

4.2 Technology trade-off for the rotor bearings

One of the central choices revolves around the design of the rotor's pivot, so that the dry friction torque can be extremely low (less than 5 µNm), including under 1-g loading for ground characterization and acceptance tests. This is incompatible with the preloaded designs generally considered for space mechanisms.

The following four candidate technologies were explored:

- Jewel bearings commonly used inside mechanical watch movements (unlubricated)
- Miniature ball bearings (with unlubricated ceramic balls, no preload)
- Magnetic suspension (passive design)
- Plain bearings (with surface treated bushings to lower the coefficient of friction)

The various pros and cons of each (in terms of friction, maturity, manufacturing/procuring and assembly cost, and robustness to mechanical/thermal environments) are summarized in the next table.

Table 3: trade-off between candidate technologies for the bearings

Technology	Pros	Cons
Jewel bearings	Very low friction	Cost (unless off-the-shelf) Low TRL for space applications
Miniature ball bearings	Low cost Easy assembly	Low heritage of unlubricated bearings for space applications
Magnetic suspension	Very low friction Low cost	Novel design Large axial play => shocks during launch Need surface treatment
Plain bearings	Lowest cost Easiest assembly	High friction under 1g Dry friction cannot be tested on ground

The plain bearing solution was discarded for not meeting the requirement of 1-g testability. The jewel bearing solution was considered too complex and not mature enough for space applications.

Two prototypes were then designed around the other two solutions (ball bearings and magnetic suspension), for preliminary performance and environment testing. The design objectives in terms of prototype representativity were focused on the bearings:

- Same rotor mass as the final flight design (~30 grams)
- Same materials and surface treatments for the bearings
- Same dimensions and manufacturing tolerances for the bearings

Figure 8: technology qualification prototypes: ball-bearing (left) / magnetic suspension (right)

4.3 Preliminary environment and performance tests

The objective was to verify that at least one technology option would withstand the harsh launch environments, while meeting the requirement in terms of dry friction, and with no noticeable change in friction *before* vs *after* the tests.

Vibration and shock tests. The requirements were taken from the Airbus standard requirements for equipment used on LEO earth observation missions:

- Sine vibration: 24 g on each axis, from 5 to 120 Hz (at 2 octaves per minute)
- Random vibration: 18.4 g RMS axial, 12.8g RMS transverse, in the range [10 2000Hz]
- Shocks: 20g at 100Hz, 2000g from 2 to 10 kHz

Friction was measured by repeatedly observing the residual angular offset when the rotor tries to realign with the local North after being rotated away.

- The ball-bearing option exhibited average friction levels noticeably above the 5 µNm goal, but still compatible with efficient detumbling (see §3.3)
- The magnetic suspension option exhibited lower friction levels, with some data points marginally above 5 µNm depending on the angular position of the rotor.

For both prototypes, no statistical evolution of the friction levels could be observed after the environment tests. Moreover, visual inspection after disassembly identified no visible damage on surfaces, confirming the robustness to design loads.

Thanks to these tests, the industrial risk is greatly reduced, since two very different technology options are now proved to be eligible. This clears the way for finalizing the development.

4.4 Upcoming tests

The second phase of the ongoing R&T with CNES will cover this qualification effort, with the detailed design and manufacturing of an EQM, for formal environment and performance testing:

- Thermal/vacuum tests
- Vibration/shock tests
- Acceptance tests: dry friction (before and after environment tests)
- Performance tests: damping coefficient k_v (before and after environment tests)

Additionally, the macroscopic detumbling function will be validated with a ground setup demonstrating the *complete physical principle*, where a dummy inertia suspended by a torsion wire acts as the spacecraft that needs detumbling. This setup was successfully used for demonstrating the same principle on a precursor design in 2018.

Meanwhile, we are actively pursuing avenues for *in-orbit demonstration*: the simplicity of the device allows to fast-track the production of a demonstration unit, should an opportunity arise early.

4.5 Adaptations for smaller satellites

Until now, the design setpoint described and tested is for k_v = 1 mNms/rad, intended for relatively large satellites. The device can however be easily adapted for smaller satellites, with minimal changes and minimum delta-qualification effort:

- Same form factor, same parts (the size is already small enough for even very small satellites)
- Smaller magnets, since the lower inertia requires a lower k_v. This reduces the disturbance torque and also the magnetic bias caused by the device (allowing to accommodate the detumbler closer to the magnetometer).

5 CONCLUSIONS AND PERSPECTIVES

5.1 Current status and development roadmap

The current development status as of mid-2023, reached after an internal R&D in 2020-2021 and a joint R&T with CNES in 2021-2023 ('Dispositif de detumbling passif', still ongoing) is the following:

- Theoretical background, simulation and sizing tools
- Experimental validation of key theoretical predictions
- Functional consolidation via detailed simulation campaigns
- Verification of innocuity with respect to the host satellite
- Trade-off on alternative technologies for the rotor bearings
- Manufacturing of two breadboards
- Vibration, shock and friction tests
- Reference sizing and design

In terms of technology readiness, TRL6 will be achieved by the end of 2023 with qualification tests on an EQM. The first flight models are expected to be ready before end-2024.

5.2 Patenting and IPR

The design of the detumbler is covered by three patents:

- 2016 – EP3538441B1 – Tourneur/Lagadec (see [2])
- 2021 – FR2110081 – Boyer/Lagadec (see [3])
- 2023 – FRXXXXX – Brault/Lagadec (pending)

5.3 Conclusions: a breakthrough for space sustainability

By guarding satellites against tumbling after the end of their operational lifetime, the detumbler makes active debris removal designs and operations much less daunting. Considering how small and inexpensive the solution is, there should be no obstacle against accommodating one such detumbler on all future LEO missions, as an insurance policy in case post-mission disposal fails.

6 REFERENCES

[1] B. Bastida Virgili, H. Krag, *Active Debris Removal for LEO Missions*, 6th European Conference on Space Debris, 2013

[2] C. Tourneur, K. Lagadec, *Spacecraft Comprising Active Attitude Control Means and Passive Attitude Control Means*, Patent ref FR3058393, WO/2018/087273, priority November 2016

[3] L. Boyer, K. Lagadec, *Device for Controlling the Angular Velocity of a Spacecraft, and Corresponding Spacecraft*. Patent ref FR2110081, WO/2023/047049, priority September 2021